Life histories and niche dynamics in late Quaternary proboscideans from midwestern North America

Chris Widga[a,b]* [iD] , Greg Hodgins[c], Kayla Kolis[d], Stacey Lengyel[a,b], Jeff Saunders[b,e], J. Douglas Walker[f], Alan D. Wanamaker[g]

[a]Don Sundquist Center of Excellence in Paleontology, East Tennessee State University, 1212 Suncrest Dr., Gray, TN, 37615
[b]Research and Collections Center, Illinois State Museum, 1011 E. Ash St., Springfield, IL, 62703
[c]Department of Physics, University of Arizona, 1118 E. Fourth St., Tucson, AZ, 85721
[d]Biodiversity Institute, University of Kansas, 1345 Jayhawk Blvd., Lawrence, KS, 66045
[e]The Desert Laboratory on Tumamoc Hill, University of Arizona, 1675 W. Anklam Rd., Tucson, AZ, 85745
[f]Department of Geology, University of Kansas, 1414 Naismuth Dr., Lawrence, KS, 66045
[g]Department of Geological and Atmospheric Sciences, Iowa State University, 253 Science, Ames, IA, 50011
*Corresponding author at: 1212 Suncrest Dr., Gray, TN 37615. E-mail address: widgac@etsu.edu (C. Widga)

Abstract

Stable isotopes of mammoths and mastodons have the potential to illuminate ecological changes in late Pleistocene landscapes and megafaunal populations as these species approached extinction. The ecological factors at play in this extinction remain unresolved, but isotopes of bone collagen (δ^{13}C, δ^{15}N) and tooth enamel (δ^{13}C, δ^{18}O, ^{87}Sr/^{86}Sr) from midwestern North America are leveraged to examine ecological and behavioral changes that occurred during the last interglacial-glacial cycle. Both species had significant C3 contributions to their diets and experienced increasing levels of niche overlap as they approached extinction. A subset of mastodons after the last glacial maximum exhibit low δ^{15}N values that may represent expansion into a novel ecological niche, perhaps densely occupied by other herbivores. Stable isotopes from serial and microsampled enamel show increasing seasonality and decreasing temperatures as mammoths transitioned from Marine Isotope Stage (MIS) 5e to glacial conditions (MIS 4, MIS 3, MIS 2). Isotopic variability in enamel suggests mobility patterns and life histories have potentially large impacts on the interpretation of their stable isotope ecology. This study further refines the ecology of midwestern mammoths and mastodons demonstrating increasing seasonality and niche overlap as they responded to landscape changes in the final millennia before extinction.

Keywords: Mammoths; Mastodons; Stable isotopes; Paleoecology; Midwest; Mobility

INTRODUCTION

Historically, the late Quaternary record of mammoths and mastodons in the Midwest has played an important role in understanding megafaunal extinctions in North America (e.g., Fisher, 2009, 2018; Saunders et al., 2010; Yansa and Adams, 2012; Widga et al., 2017a). Whether extinctions are viewed as human induced (Mosimann and Martin, 1975; Alroy, 2001; Surovell et al., 2005, 2016; Fisher, 2009), the result of late Pleistocene landscape changes (Stuart et al., 2004; Nogués-Bravo et al., 2008; Widga et al., 2017a), a function of other ecological processes (Ripple and Van Valkenburgh, 2010), or some combination, this region is

unparalleled in its density of large late Quaternary vertebrates and associated paleoecological localities. For these reasons, the midcontinent has proven critical in understanding ecological dynamics in proboscidean taxa leading up to extinction. In recent years, it has been recognized that multiple proboscidean taxa shared an ecological niche in late Pleistocene landscapes (Saunders et al., 2010), despite distinct extinction trajectories (Widga et al., 2017a). Chronological studies indicate that proboscideans in this region experienced extinction in situ, rather than mobilizing to follow preferred niche space (Saunders et al., 2010). Despite refinements in our understanding of mammoths and mastodons in the region, many significant questions remain. Modern megafauna have a profound impact on local vegetation (Guldemond and Van Aarde, 2008; Valeix et al., 2011), and it is unclear what effect late Pleistocene mammoths and mastodons would have had on canopy cover, nutrient cycling, and fruit dispersal in non-analogue vegetation communities. There are still issues of

Table 1. Temporal scale in paleoecological analyses.

Scale	Method	Phenomena	Selected references
Small (days)	Stomach contents, enamel microwear	Animal health, landscape (local scale)	Rhodes et al., 1998; Teale and Miller 2012; Green et al., 2017; Smith and DeSantis, 2018
Meso (weeks–months)	Hair, tusk/tooth dentin, tooth enamel	Seasonal diets, reproductive events (e.g., musth, calving), migration/dispersal	Fox and Fisher, 2001; Hoppe, 2004; Hoppe and Koch, 2007; Cerling et al., 2009; Metcalfe and Longstaffe, 2012; Fisher, 2018
Large (years–decades)	Bone collagen, tooth enamel, tooth mesowear	Climate/vegetation trends, large-scale land-use trends, population-level trends in diet, responses to landscape changes	Bocherens et al., 1996; Iacumin et al., 2010; Szpak et al., 2010

equifinality in how the presence of human predators (Fisher, 2009) or the absence of both humans and large carnivores (Widga et al., 2017a) impacted proboscidean populations in the region as they neared extinction.

The high-profile debate surrounding the cause of late Pleistocene megafaunal extinctions spurred several productive regional studies to address the timing and paleoecology of extinction in megafaunal taxa (Pacher and Stuart, 2009; Stuart and Lister, 2011, 2012; Stuart, 2015; Widga et al., 2017a). The results of this research serve to constrain the number of possible extinction scenarios and highlight the need for regional-scale and taxon-specific analyses.

As in modern ecosystems, Proboscidea in late Pleistocene North America were long-lived taxa that likely had a profound impact on the landscape around them. Owing to their size and energetic requirements, elephantoids are a disruptive ecological force, promoting open canopies in forests through tree destruction (Chafota and Owen-Smith, 2009) and trampling vegetation (Plumptre, 1994). Their dung is a key component of soil nutrient cycling (Owen-Smith, 1992; Augustine et al., 2003) and was likely even more important in nitrogen-limited tundra and boreal forest systems of temperate areas during the late Pleistocene. Even in death, mammoths and mastodons probably wrought major changes on the systems in which they were interred (Coe, 1978; Keenan et al., 2018), providing valuable nutrient resources to scavengers and microbial communities. Precisely because proboscideans play such varied and important roles in the ecosystems they inhabit, they are good study taxa to better understand Pleistocene ecosystems. They are also central players in many extinction scenarios.

One of the major challenges to ecological questions such as these is scale (Delcourt and Delcourt, 1991; Denny et al., 2004; Davis and Pineda-Munoz, 2016). Processes that are acting at the level of an individual or a locality can vary significantly in space and time (Table 1). Paleoecological data collected from individual animals from local sites are constrained by larger regional patterns that may or may not be apparent (e.g., taphonomic contexts, predator-prey dynamics). Paleoecological studies of vertebrate taxa often begin with the premise that the individual is an archive of environmental phenomena experienced in life. In long-lived taxa such as proboscideans, this window into past landscapes may span many decades. This longevity is both a benefit and a challenge to studies of proboscidean paleoecology.

Some approaches offer relatively high-resolution snapshots of animal ecology at a scale that is of a short duration (days). Microwear analyses of dentin and enamel (Green et al., 2017; Smith and DeSantis, 2018) are increasingly sophisticated and have the potential to track short-term dietary trends. The remains of stomach contents—essentially the "last meal" representing a few hours of individual browsing—also provide ecological information at this scale (Lepper et al., 1991; Newsom and Mihlbachler, 2006; van Geel et al., 2011; Fisher et al., 2012; Teale and Miller, 2012; Birks et al., 2019). These techniques offer paleoecological insights that are minimally time-averaged and at a timescale that may be comparable to modern observations of animal behavior.

Other approaches resolve time periods that are weeks to months in duration. Fisher's work on incremental growth structures in proboscidean tusk and molar dentin reliably records weekly to monthly behaviors (Fisher and Fox, 2006; Fisher, 2009, 2018). The resolution of these methods may even include short-term, often periodic, life history events, such as reproductive competition (musth) and calving. Other researchers (Hoppe et al., 1999; Metcalfe and Longstaffe, 2012, 2014; Pérez-Crespo et al., 2016) have explored incremental growth trends in proboscidean tooth enamel. Adult molars form over the course of 10–12 years with an enamel extension rate of ~1 cm/year in modern elephants (Uno et al., 2013) and mammoths (Dirks et al., 2012; Metcalfe and Longstaffe, 2012), providing the opportunity to understand mesoscale (potentially monthly) changes in diet and behavior.

Finally, some techniques measure animal diet and behavior over much longer scales (years–decades). In humans, bone collagen is replaced at a rate of 1.5–4% per year (Hedges et al., 2007). For equally long-lived proboscideans, and assuming a similar rate of collagen replacement, this means that stable isotope analyses of bone collagen is essentially sampling a moving average of ~20 years of animal growth. For younger age groups, this average will be weighted toward time periods of accelerated maturation (adolescence), when collagen is replaced at a much greater rate (Hedges et al., 2007). Tooth enamel can also be sampled at a resolution (i.e., "bulk" enamel) that averages a year (or more) of growth (Hoppe, 2004; Baumann and Crowley, 2015), and it is likely that this is the approximate temporal scale that is controlling tooth mesowear (Fortelius and Solounias, 2000).

Stable isotope studies are an important part of the paleo-ecological toolkit for understanding Quaternary proboscideans and are capable of resolving animal behavior at multiple timescales. Progressively larger, more complete datasets characterize isotopic studies of Beringian mammoths, where stable carbon and oxygen isotopes in bone collagen and tooth enamel reliably track climate and landscape changes throughout the late Pleistocene (Bocherens et al., 1996; Iacumin et al., 2010; Szpak et al., 2010; Arppe et al., 2019), the place of mammoths in regional food webs (Fox-Dobbs et al., 2007, 2008), and characteristics of animal growth and maturation (Metcalfe and Longstaffe, 2012; Rountrey et al., 2012; El Adli et al., 2017).

These studies have also been important in understanding both lineages of proboscideans in temperate North America. From the West Coast (Coltrain et al., 2004; El Adli et al., 2015) to the southwestern (Metcalfe et al., 2011) and eastern United States (Koch et al., 1998; Hoppe and Koch, 2007), isotopic approaches have been very successful in understanding local- to regional-scale behavior in mammoths and mastodons. Although there have been efforts to understand mammoth and mastodon behaviors in the Midwest at relatively limited geographic scales (Saunders et al., 2010; Baumann and Crowley, 2015), there is a need to systematically address long-term isotopic trends throughout the region. In this paper, we approach this problem from a broad regional perspective, leveraging a recently reported radiocarbon (^{14}C) dataset with associated isotopic data on bone collagen. We also utilize an enamel dataset consisting of both serial bulk and micromilled mammoth molar enamel samples (C, O, Sr isotope systems). Together, the results of these analyses offer a picture of mammoth and mastodon diets (δ^{13}C, δ^{15}N), late Quaternary paleoclimate (δ^{18}O), and animal mobility (^{87}Sr/^{86}Sr) that is geographically comprehensive and spans the past 50,000 years.

MATERIALS AND METHODS

The proboscidean dataset in this study (Fig. 1, Supplementary Tables 1–3) was acquired with the goal of understanding mammoth and mastodon population dynamics during the late Pleistocene, as these taxa approached extinction. Chronological and broad-scale paleoecological implications for this dataset were explored in Widga et al. (2017a) and more recently in Broughton and Weitzel (2018). In this paper, we focus on the implications of these data for the stable isotope ecology of midwestern Proboscidea. We also discuss annual patterns in five serially sampled mammoth teeth spanning the last glacial-interglacial cycle. Finally, we microsampled two mammoths from the Jones Spring locality in Hickory County, Missouri. Although beyond the range of radiocarbon dating, both samples are associated with well-dated stratigraphic contexts (Haynes, 1985). Specimen 305JS77 is an enamel ridge-plate recovered from unit d1 (spring feeder), refitting to an M3 from unit c2 (lower peat). Unit c2 is part of the lower Trolinger Formation (Haynes, 1985) and can be assigned to Marine Isotope Stage (MIS) 4. Specimen 64JS73 is an enamel ridge-plate from unit e2 (sandy peat) in the upper Trolinger Formation (Haynes, 1985) and can be assigned to MIS 3. Together, these samples provide dozens of seasonally calibrated isotopic snapshots representing mammoth behavior from individuals that predate the last glacial maximum (LGM).

Mammoth and mastodon bone collagen

Proboscidean samples were selected to widely sample midwestern Proboscidea, both stratigraphically and geographically (Widga et al., 2017a). Owing to extensive late Pleistocene glaciation in the region, this dataset is dominated by samples dating to the LGM or younger (<22 ka). Only 14 out of 93 (15%) localities predate the LGM.

All samples were removed from dense bone and tooth or tusk dentin and submitted to the University of Arizona AMS Laboratory. Collagen was prepared using standard acid-base-acid (ABA) techniques (Brock et al., 2010); its quality was evaluated visually and through ancillary Carbon:Nitrogen (C:N) analyses (Supplementary Table 1). Visually, well-preserved collagen has a white, fluffy appearance and C:N ratios within the range of modern bones (2.9–3.6) (Tuross et al., 1988). Samples outside this range were not included in the study. Samples that had the potential to be terminal ages were subjected to additional analyses where the ABA-extracted gelatin was ultrafiltered through >30 kD syringe filters to isolate relatively undegraded protein chains (Higham et al., 2006). This fraction was also dated. All radiocarbon ages in this dataset are on collagen from proboscidean bone or tooth dentin and available in Widga et al. (2017a), through the Neotoma Paleoecology Database (www.neotomadb.org), and in Supplementary Table 1. Measured radiocarbon ages were calibrated in Oxcal v. 4.3 (Bronk Ramsey, 2009), using the Intcal13 dataset (Reimer et al., 2013). All stable isotope samples were analyzed on a Finnigan Delta PlusXL continuous-flow gas-ratio mass spectrometer coupled to a Costech elemental analyzer at the University of Arizona. Standardization is based on acetanilide for elemental concentration, NBS-22 and USGS-24 for δ^{13}C, and IAEA-N-1 and IAEA-N-2 for δ^{15}N. Isotopic corrections were done using a regression method based on two isotopic standards. The long-term analytical precision (at 1σ) is better than ± 0.1‰ for δ^{13}C and ± 0.2‰ for δ^{15}N. All δ^{13}C results are reported relative to Vienna Pee Dee Belemnite (VPDB), and all δ^{15}N results are reported relative to N-AIR

Serial and microsampling of mammoth tooth enamel

Mammoth enamel ridge-plates were sampled at two different scales. Serial sampling consisted of milling a series of 5–10 mg samples of enamel powder with a handheld rotary tool equipped with a 1.5-mm-diameter carbide bit along the axis of growth. Sample spacing was approximately one sample per centimeter of tooth growth. However, given the geometry and timing of enamel maturation (Dirks et al., 2012), these
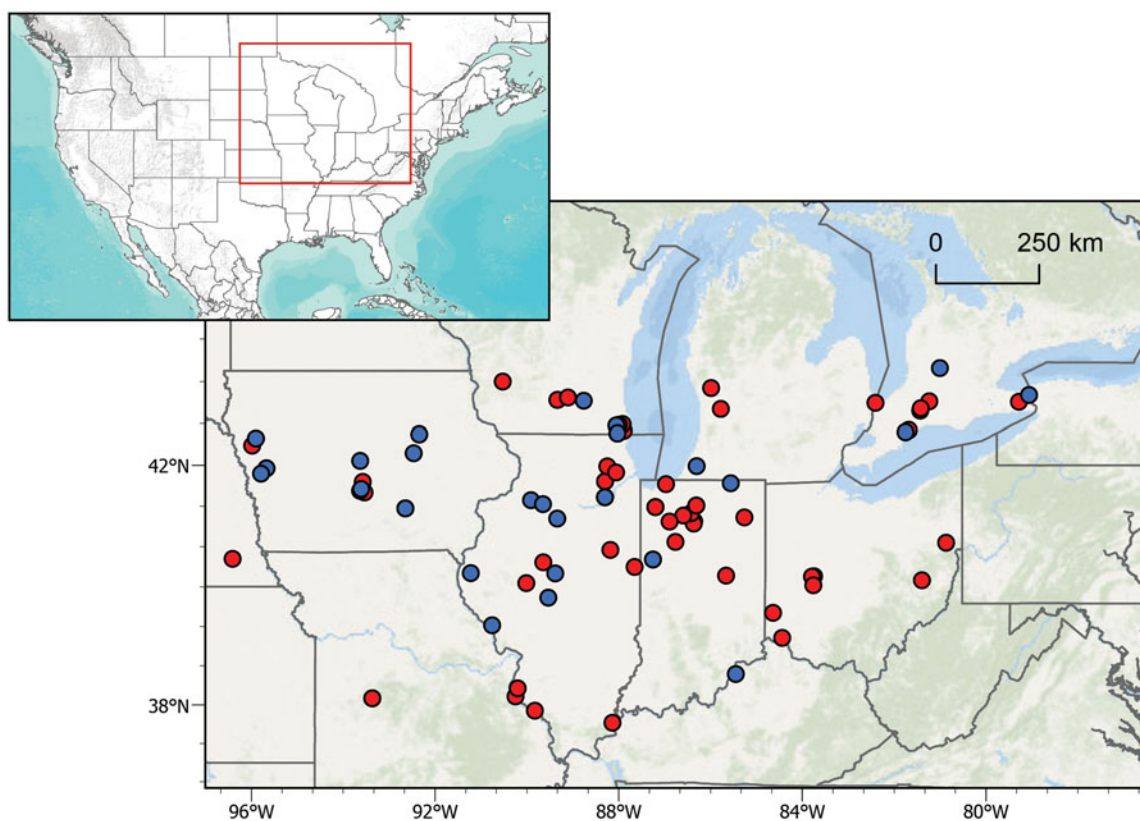
Figure 1. Locations of dated midwestern mammoths (blue circles) and mastodons (red circles) with associated $\delta^{13}C_{coll}$ and $\delta^{15}N_{coll}$ data. See Supplementary Table 1 for details. (For interpretation of the references to color in this figure legend, the reader is referred to the web version of this article.)

samples at best approximate an annual scale of dietary and water inputs.

Microsampling, however, has the potential to record sub-annual patterns in animal movement and behavior (Metcalfe and Longstaffe, 2012). For this project, we built a custom micromill capable of in situ, micron-resolution, vertical sampling of a complete mammoth molar. This micromill setup consisted of two Newmark linear stages coupled to a Newmark vertical stage to allow movement in three dimensions. These stages were controlled by a Newmark NSC-G 3-axis motion controller using GalilTools on a PC. A 4-cm-diameter ball joint allowed leveling of a metal (version 1) or acrylic (version 2) plate for holding a specimen. The armature for version 1 consisted of a 1971 Olympus Vanox microscope retrofitted with a stationary Proxxon 50/E rotary tool using a 0.5-mm end mill. Version 2 replaced this setup with a U-strut armature using a 3D printed drill mount to allow for greater vertical and horizontal movement to accommodate large, organically shaped specimens. Specimens were stabilized on the mounting plate using a heat-flexible thermoplastic cradle affixed to a metal plate with machine screws (version 1). However, we later developed an acrylic mounting plate method where a mammoth tooth could be sufficiently stabilized using zip ties (version 2). This micromill was developed to address the challenges of accurately micromilling large specimens with minimal instrumentation costs.

Complete plans for this micromill are available under an open hardware license at https://osf.io/8uhqd/?view_only=43b4242623a94a529e4c6ef2396345e9.

Micromill sampling resolution was one sample per millimeter along the growth axis of the tooth-plate (Fig. 2). Each sample was milled in 100 μm deep passes through the entire thickness of the enamel. The lowest enamel sample (i.e., closest to the enamel-dentin boundary) in the series was used for isotopic analyses to minimize the effects of mineralization and diagenesis on the biological signal (Zazzo et al., 2006). Enamel powder was collected in deionized water to maximize sample recovery and lubricate the mill. These samples were too small for standard pretreatment of tooth enamel carbonate (Koch et al., 1997). However, paired bulk enamel samples treated with 0.1 N acetic acid and 2.5% NaOCl showed results that are the same as untreated bulk samples (see Supplemental Material). Although this technique is both time- and labor-intensive, it is minimally invasive and is capable of sampling enamel growth structures at high resolution.

All enamel powder samples were measured in a Finnigan Delta Plus XL mass spectrometer in continuous-flow mode connected to a gas bench with a CombiPAL autosampler at the Iowa State University Stable Isotope Laboratory, Department of Geological and Atmospheric Sciences. Reference standards (NBS-18, NBS-19) were used for isotopic

corrections and to assign the data to the appropriate isotopic scale. Corrections were done using a regression method using NBS-18 and NBS-19. Isotope results are reported in per mil (‰). The long-term precision (at 1σ) of the mass spectrometer is ± 0.09‰ for $\delta^{18}O$ and ± 0.06‰ for $\delta^{13}C$, respectively, and precision was not compromised with small carbonate samples (~150 μg). Both $\delta^{13}C$ and $\delta^{18}O$ are reported relative to VPDB.

Enamel $\delta^{13}C$ results were corrected to -14.1‰ to approximate the $\delta^{13}C$ of dietary input ($\delta^{13}C_{diet}$) (Bryant and Froelich, 1995).

Enamel $\delta^{18}O$ results were converted from VPDB to Standard Mean Ocean Water (SMOW) using the equation:

$$\delta^{18}O \; SMOW = (1.03086 * \delta^{18}O \; VPDB) + 30.86$$

The $\delta^{18}O$ of enamel phosphate ($\delta^{18}O_p$) for these samples was calculated from the $\delta^{18}O$ of enamel carbonate ($\delta^{18}O_c$) following Fox and Fisher (2001):

$$\delta^{18}O_p = (\delta^{18}O_c/1.106) - 4.7288$$

Estimates of body water $\delta^{18}O$ ($\delta^{18}O_w$) were calculated following Daux et al. (2008):

$$\delta^{18}O_w = (1.54 * \delta^{18}O_p) - 33.72$$

The $^{87}Sr/^{86}Sr$ component of enamel bioapatite reflects changes in the geochemical makeup of the surface on which an animal grazed during tooth formation. In the serial-scale analyses, enamel powder samples were split from the light isotope samples described above and represent the same portions of mammoth teeth. Each ~5 mg sample of powder was leached in 500 μL 0.1 N acetic acid for four hours to remove diagenetic calcite and rinsed three times with deionized water (centrifuging between each rinse). In the micromilled series, small sample sizes prevented Sr analyses from being performed on the same samples as $\delta^{13}C$ and $\delta^{18}O$ analyses. Therefore, Sr from these growth series was analyzed opportunistically, or at the scale of one sample every 2 mm.

All enamel samples were then dissolved in 7.5 N HNO₃ and the Sr eluted through ion-exchange columns filled with strontium-spec resin at the University of Kansas Isotope Geochemistry Laboratory. $^{87}Sr/^{86}Sr$ ratios were measured on a thermal ionization mass spectrometer, an automated VG Sector 54 eight-collector system with a 20-sample turret, at the University of Kansas Isotope Geochemistry Laboratory. Isotope ratios were adjusted to correspond to a value of 0.71250 on NBS-987 for $^{87}Sr/^{86}Sr$. We also assumed a value of $^{86}Sr/^{88}Sr$ of 0.1194 to correct for fractionation.

The distribution of $^{87}Sr/^{86}Sr$ values in vegetation across the surface of the midcontinent is determined by the values of soil parent material. In a large part of this region, surface materials are composed of allochthonous Quaternary deposits such as loess, alluvium, and glacial debris. Therefore, continent-scale

Sr isoscape models derived from bedrock or water (Bataille and Bowen, 2012) are not ideal for understanding first-order variability in midwestern $^{87}Sr/^{86}Sr$. For these reasons, Widga et al. (2017b) proposed a Sr isoscape for the Midwest based on surface vegetation. At a regional scale, these trends in vegetation $^{87}Sr/^{86}Sr$ reflect the Quaternary history of the region and are consistent with other empirically derived patterns in Sr isotope distribution from the area (Slater et al., 2014; Hedman et al., 2018). Sr isotope values in mammoth enamel are compared to a $^{87}Sr/^{86}Sr$ isoscape constructed from the combined datasets of Widga et al. (2017b) and Hedman et al. (2009, 2018).

RESULTS

The collagen of 54 mastodons and 22 mammoths was analyzed for $\delta^{13}C_{coll}$ and $\delta^{15}N_{coll}$ (Table 2). Three mastodons have ^{14}C ages that place them beyond the range of radiocarbon dating, and the youngest mastodons date to the early part of the Younger Dryas, shortly before extinction. Despite being well represented prior to the LGM and during deglaciation (i.e., Oldest Dryas, Bølling, Allerød, Younger Dryas), this dataset lacks mastodons from the study region during the coldest parts of the LGM. Mammoths are present in this dataset from 40 ka until their extinction in the region during the late Allerød.

There is a substantial amount of overlap in the $\delta^{13}C_{coll}$ and $\delta^{15}N_{coll}$ of mammoths and mastodons through the duration of the dataset (Fig. 3, Table 2). Both taxa show average $\delta^{13}C_{coll}$ values around -21‰, consistent with a diet dominated by C3 trees, shrubs, or cool-season grasses. This is broadly consistent with variable but shared diets during time periods when both taxa occupied the region. The average $\delta^{13}C_{coll}$ values for mammoths (-20.4‰; s.d. = 1.0) is similar to that for mastodons (-21.0‰; s.d. = 0.7). The average $\delta^{15}N_{coll}$ for mammoths (7.5‰; s.d. = 1.3) is elevated compared to mastodons (4.4‰; s.d. = 2.0).

However, dietary relationships between taxa are not static through time. Prior to the LGM, both $\delta^{13}C_{coll}$ and $\delta^{15}N_{coll}$ are significantly different between mammoths and mastodons ($\delta^{13}C$ t-test; $P = 0.013$; $\delta^{15}N$ t-test; $P = 0.010$). During the Oldest Dryas, the $\delta^{13}C_{coll}$ of both taxa is very similar, although $\delta^{15}N_{coll}$ between mammoths and mastodons remains distinct (t-test; $P = 0.012$). During the Allerød, $\delta^{13}C_{coll}$ and $\delta^{15}N_{coll}$ between taxa are indistinguishable.

The $\delta^{13}C_{coll}$ signature of mastodon diets changes little throughout the last 50 ka. Despite a noticeable absence of mastodon material during the height of the LGM, the only significant shift in the $\delta^{13}C_{coll}$ of mastodon diets occurs between the Bølling and the Allerød (t-test; $P = 0.008$).

Mastodon $\delta^{15}N_{coll}$ values fall clearly into two groups: those that date prior to the LGM, and those that postdate the LGM. Mastodon $\delta^{15}N_{coll}$ values are significantly higher in pre-LGM samples than in samples dating to the Younger Dryas (t-test; $P = 0.010$), Allerød (t-test; $P = 0.017$), and Bølling (t-test; $P < 0.000$). Of note is a group of mastodons that show lower $\delta^{15}N_{coll}$ values during the Oldest Dryas,
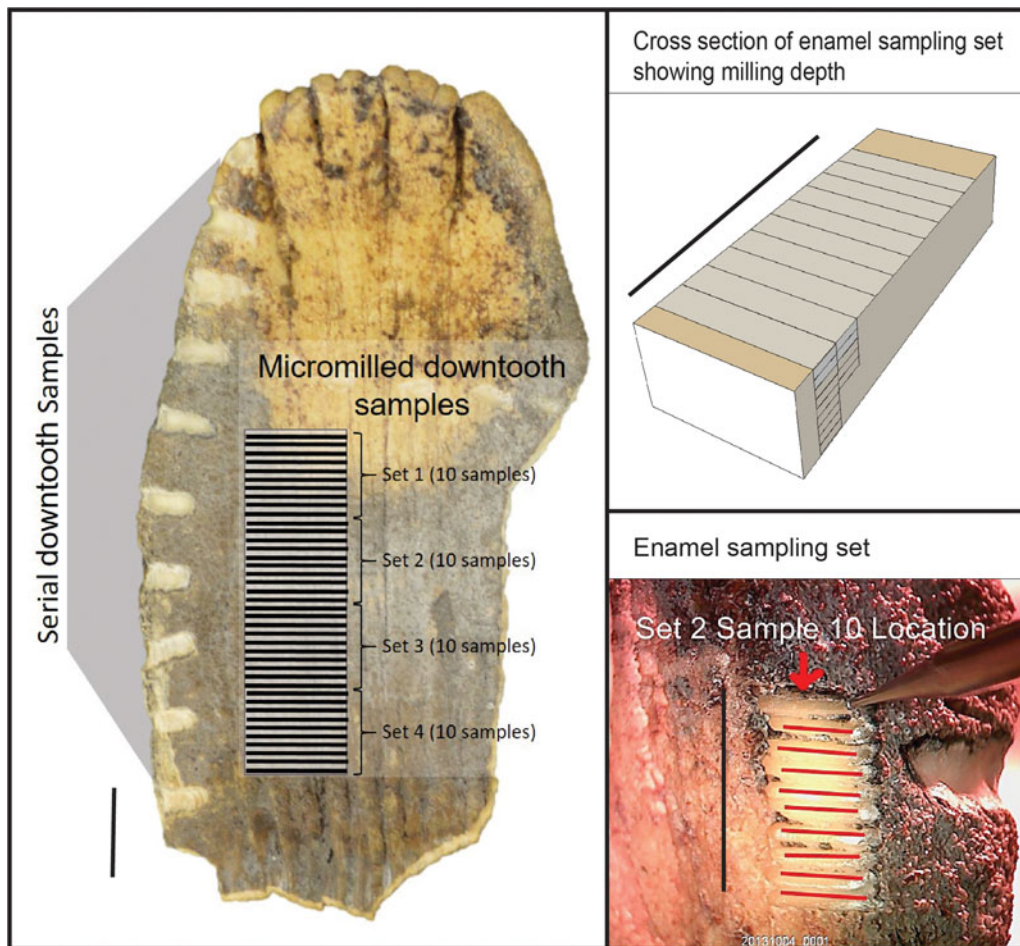
**Figure 2.** (color online) Schematic illustration of serial and microsampling strategies. Black bar = 1 cm.

Table 2. Mastodon and mammoth collagen stable isotope values, by chronozone. $\delta^{13}C$ values are reported as ‰ relative to VPDB. $\delta^{15}N$ values are reported as ‰ relative to AIR.

Taxon	Chronozone	N	$\bar{x}\,\delta^{13}C$ (s.d.)	$\bar{x}\,\delta^{15}N$ (s.d.)
Mammut	Younger Dryas (12.9–11.5 ka)	2	−20.6 (0.4)	2.9 (0.6)
	Allerød (14.0–12.9 ka)	35	−21.1 (0.6)	4.2 (2.1)
	Bølling (14.6–14.0 ka)	6	−20.4 (0.5)	3.8 (1.5)
	Oldest Dryas (14.6–17.4 ka)	5	−20.5 (0.7)	4.6 (1.6)
	LGM II (17.4–20.9 ka)	0		
	LGM I (20.9–22.9 ka)	0		
	Pre-LGM (>22.9 ka)	6	−20.9 (0.7)	6.1 (1.3)
	Average	54	−21.0 (0.7)	4.4 (2.0)
Mammuthus	Allerød (14.0–12.9 ka)	3	−20.6 (0.9)	6.1 (2.0)
	Bølling (14.6–14.0 ka)	1	−19.9	5.8
	Oldest Dryas (14.6–17.4 ka)	4	−21.4 (0.5)	7.9 (1.3)
	LGM II (17.4–20.9 ka)	4	−21.1 (0.4)	7.4 (1.3)
	LGM I (20.9–22.9 ka)	5	−20.1 (1.1)	7.6 (1.2)
	Pre-LGM (>22.9 ka)	5	−19.6 (0.8)	8.2 (0.7)
	Average	22	−20.4 (1.0)	7.5 (1.3)

Bølling, Allerød, and Younger Dryas, when the average $\delta^{15}N_{coll}$ values decrease to values <5‰. A similar shift is not evident in mammoths at this time.

Mammoth $\delta^{13}C_{coll}$ during MIS 3 is significantly different from mammoths dating to LGM II (*t*-test; *P* = 0.008) or the Oldest Dryas (*t*-test; *P* = 0.005). There are no significant differences in mammoth $\delta^{15}N_{coll}$ between different time periods.
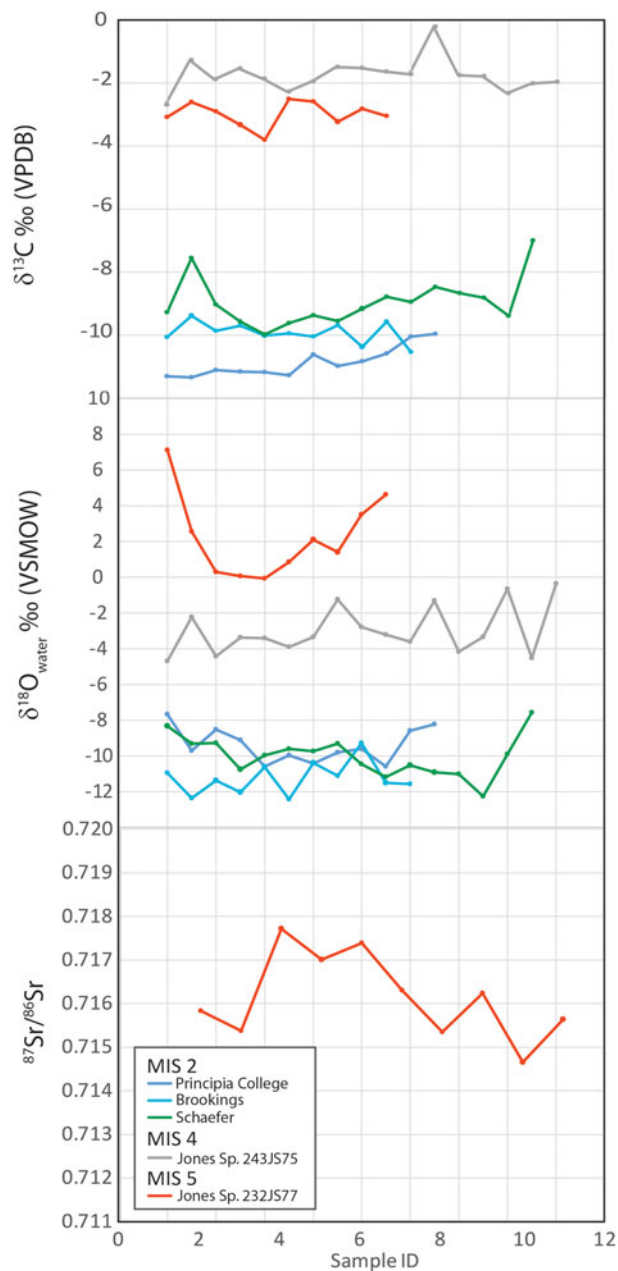
All serial enamel series were between 9 and 16 cm in length and represent multiple years. Stable oxygen isotopes of three MIS 2 mammoths (Principia College, Brookings, Schaeffer) overlap significantly, while MIS 4 (234JS75) and MIS 5e (232JS77) mammoths from Jones Spring show elevated values indicative of warmer conditions (Fig. 4, Table 3). The variance in serially sampled MIS 2 mammoths (average amplitude = 2.5‰) was not significantly different from the series from Jones Spring, dating to MIS 4 (amplitude = 2.9‰) (*F*-test; *P* = 0.320). However, the MIS 5e mammoth from Jones Spring has a smaller amplitude (1.1‰) compared to the MIS 4 mammoth (*F*-test; *P* = 0.003) and the three MIS 2 mammoths (*F*-test; *P* < 0.000). Strontium isotope ratios of this animal indicate a home range on older, more weathered surfaces of the Ozarks throughout tooth formation, with a period of relatively elevated $^{87}Sr/^{86}Sr$ values also corresponding to low $\delta^{18}O$ values.
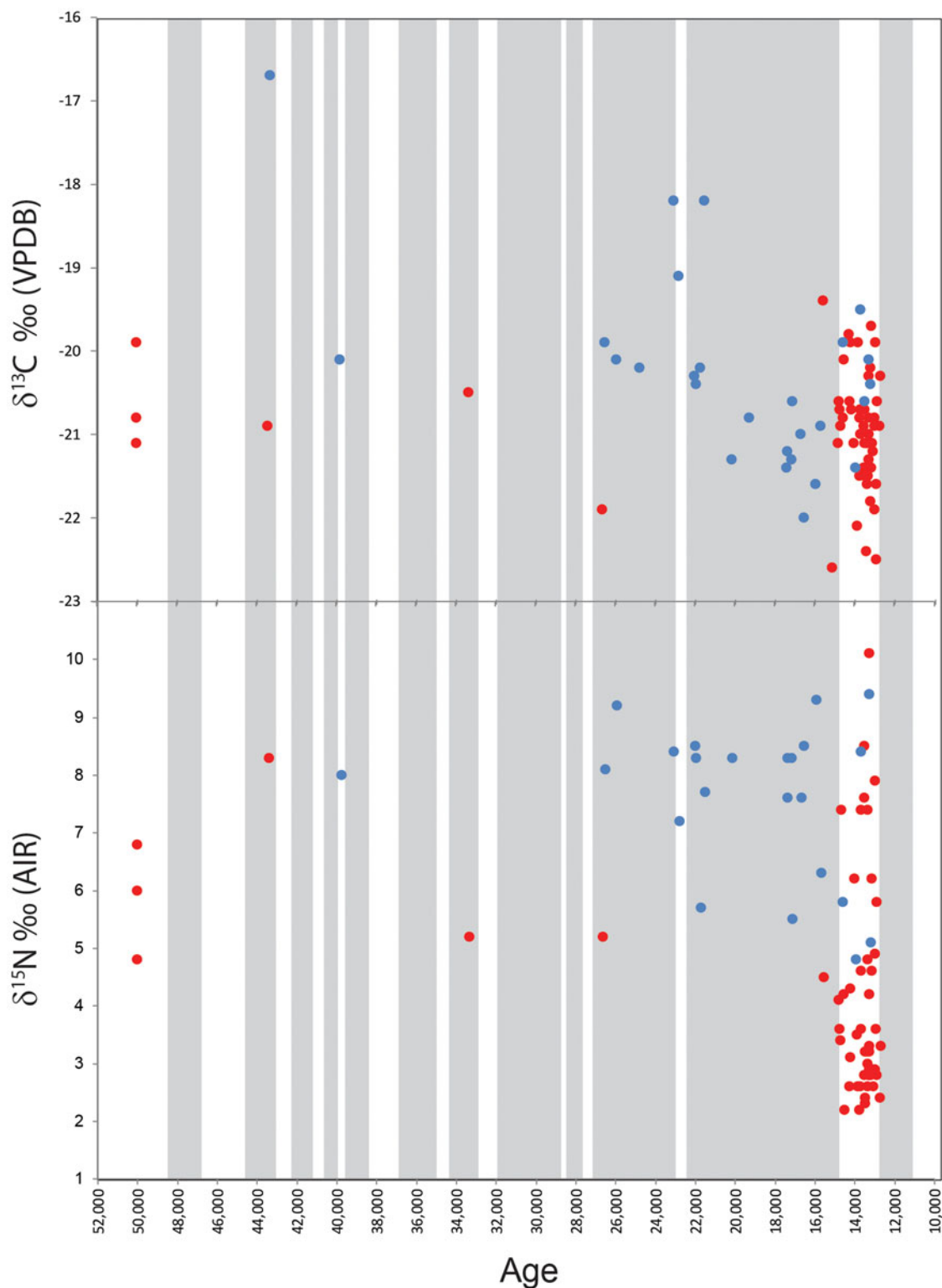
Figure 3. Changes in midwestern proboscidean collagen $\delta^{13}C$ and $\delta^{15}N$ through time, showing mastodons (red circles), mammoths (blue circles), and glacial stadials (gray bars). Specimen age is from Supplementary Table 3. Stadial chronology is from Rasmussen et al. (2014). (For interpretation of the references to color in this figure legend, the reader is referred to the web version of this article.)

Two mammoth teeth from Jones Spring were micro-sampled (Fig. 5). These specimens are from beds representative of MIS 4 and MIS 3 deposits.

The MIS 3 molar (64JS73) shows regular negative excursions in $\delta^{18}O$ values. These excursions are relatively short-lived and extreme. Considering the comparatively small analytical

Figure 4. (color online) Time series, serial enamel δ^{13}C, δ^{18}O, and ^{87}Sr/^{86}Sr.

The ^{87}Sr/^{86}Sr isotope series from both animals demonstrate an adherence to separate home ranges (Fig. 6). The MIS 4 mammoth shows values similar to bedrock units outcropping locally in central-western Missouri and neighboring areas of Kansas and Oklahoma. The MIS 3 mammoth, however, had a home range across rock units with much higher ^{87}Sr/^{86}Sr values. The home ranges for these animals do not overlap, despite their recovery from different strata within the same locality.

DISCUSSION

Despite overall similar isotopic values in mammoths and mastodons throughout the period of this study, underlying nuances are informative to regional changes in niche structure and climate. The absence of dated mastodons during the coldest parts of the LGM suggests that *Mammut* was, at least to some degree, sensitive to colder climates and adjusted its range accordingly.

Comparisons between coeval mammoths and mastodons indicate a gradual collapse of niche structure. Prior to MIS 2, δ^{13}C$_{coll}$ and δ^{15}N$_{coll}$ values between taxa were significantly different. By the end of the Allerød, mammoth and mastodon diets were isotopically indistinguishable.

Through time, there was no significant change in the δ^{13}C$_{coll}$ of mastodons. Although average mammoth δ^{13}C$_{coll}$ in the region during the latter part of the LGM was slightly more negative than in other time periods, this is not a marked shift and may be a function of decreased partial pressure of carbon dioxide during that time (Schubert and Jahren, 2015). Globally, Siberian and European mammoths exhibit a similar range of δ^{13}C$_{coll}$ values (Iacumin et al., 2010; Szpak et al., 2010; Arppe et al., 2019; Schwartz-Narbonne et al., 2019).

In both taxa, mean δ^{15}N$_{coll}$ decreases slightly throughout the sequence; however, the minimum δ^{15}N values for mastodons during the Bølling, Allerød, and Younger Dryas are significantly lower than for earlier mastodons. The anomalously low values of these late mastodons are also shared with other published mastodon values in the Great Lakes region (Metcalfe et al., 2013). They are also significantly lower than contemporary midwestern, Eurasian or Beringean mammoths (with some exceptions; see Drucker et al., 2018). The timing of these low mastodon δ^{15}N$_{coll}$ values corresponds to regionally low δ^{15}N$_{coll}$ values in the bone collagen of nonproboscidean taxa from European late Quaternary contexts (Richards and Hedges, 2003; Stevens et al., 2008; Drucker et al., 2009; Rabanus-Wallace et al., 2017), suggesting broad changes in global climate may have had cascading impacts in the nitrogen budget of local ecosystems.

Understanding in more detail how climate might have affected N cycling in midwestern ecosystems remains unclear. Flux in soil and plant N may be a function of plant-based N_2 fixation (Shearer and Kohl, 1993), rooting depth (Schulze et al., 1994), N loss related to climate factors (Handley and Raven, 1992; Austin and Vitousek, 1998), microbial activity, or mycorrhizal colonization (Michelsen et al., 1998; Hobbie et al., 2000). Furthermore, the role of large herbivore populations in N flux may be significant (Frank et al., 2004).

uncertainty (± 0.09‰), we interpret these data as reflecting seasonal changes in ingested water. This is consistent with δ^{18}O in enamel series of other hypsodont mammals, such as bison and horses (Higgins and MacFadden, 2004; Feranec et al., 2009; Widga et al., 2010). Seasonal variation in enamel growth rate and maturation may account for the perceived short length of these periods. Maximum δ^{18}O values in both mammoths are similar, however; the MIS 4 mammoth lacks these negative excursions and exhibits values that are more complacent through the length of the tooth. The δ^{13}C series from both molars indicate these mammoths experienced a C4 diet throughout the year. However, deep dips in the δ^{18}O series of the MIS 3 molar also correspond to at least two temporary peaks in the δ^{13}C series.

Table 3. Summary of serial and microsampled *Mammuthus* tooth enamel: $\delta^{13}C$, $\delta^{18}O$, and $^{87}Sr/^{86}Sr$.

| ID Serial Analyses	$\delta^{13}C$				$\delta^{18}O$				$^{87}Sr/^{86}Sr$			
	$\bar{x}$	Min	Max	Amp	$\bar{x}$	Min	Max	Amp	$\bar{x}$	Min	Max	Amp
Principia College (MIS 2)	−10.9	−11.3	−10.0	1.4	−7.9	−8.7	−6.7	2.0				
Brookings Mammoth (MIS 2)	−9.9	−10.5	−9.4	1.1	−9.2	−10.0	−7.8	2.2				
Schaefer Mammoth (MIS 2)	−9.0	−9.9	−7.0	3.0	−8.3	−9.9	−6.6	3.3				
Jones Sp. Mammoth, 243JS75 (MIS 4)	−1.7	−2.3	−0.2	2.1	−3.4	−4.5	−1.6	2.9				
Jones Sp. Mammoth, 232JS77 (MIS 5e)	−2.8	−3.8	−1.3	2.5	−0.5	−4.6	3.6	1.1	0.7162	0.7146	0.7177	0.0031
Microanalyses												
305JS77 (MIS 4)	−2.4	−3.5	−0.2	3.3	−3.9	−4.9	−2.9	2.0	0.7109	0.7106	0.7118	0.0012
64JS73 (MIS 3)	−2.8	−4.3	−1.7	2.6	−4.9	−12.0	−0.4	11.7	0.7152	0.7140	0.7164	0.0024

In N-limited environments such as tundra, terrestrial plants may receive relatively more N from inorganic sources. Boreal forests like those of the Midwest during the Bølling and Allerød, however, exhibit relatively greater biological productivity, so plant shoots are more likely to take in volatized ammonia (low $\delta^{15}N$) from organic sources such as urea (Fujiyoshi et al., 2017).

At this time, it is difficult to distinguish which (if any) of these factors had an impact on late Quaternary mastodon $\delta^{15}N_{coll}$ values. Although there is a wide range in $\delta^{15}N_{coll}$ of mammoths and mastodons throughout the sequence, $\delta^{15}N_{coll}$ values below 5‰ are only present in mastodons during post-LGM deglaciation in the lower Great Lakes (39–43° latitude), throughout an area suggested to be vegetated by a disharmonious flora dominated by black ash and spruce (Gill et al., 2009; Gonzales and Grimm, 2009) (Fig. 7). The low $\delta^{15}N_{coll}$ values suggest that these mastodons occupied an undefined, local-scale dietary niche that was not shared by contemporary mammoths or by earlier mastodons. Previous research has suggested that the Bølling-Allerød may have been a time of high mastodon populations in the Great Lakes region (Widga et al., 2017a). The concentration of mastodons around water sources may have had an impact on the $\delta^{15}N$ of browsed plants owing to increased contributions of herbivore urea. Isotopically light plant shoots can occur with increased utilization of volatized NH_4 from organic sources, including urea from herbivores.

Life histories of midwestern mammoths

Through analyses of incremental growth structures in mammoths, such as molar enamel or tusk dentin, we can reconstruct longitudinal life histories that reflect the landscape experienced by an animal over multiple years. Late Pleistocene mammoths from the study region exhibit relatively consistent downtooth patterns in $\delta^{13}C$ and $\delta^{18}O$. Similar bulk enamel isotope values in South Dakota, Wisconsin, and Illinois mammoths suggest access to broadly similar resources and relatively stable access to these resources across multiple years of the life of an individual (Fig. 4). Less negative $\delta^{13}C$ and $\delta^{18}O$ values in the last forming samples of the Schaeffer mammoth suggest a change in that animal's life history in the year before death. This change could be explained by local environmental changes resulting in nutritional stress.
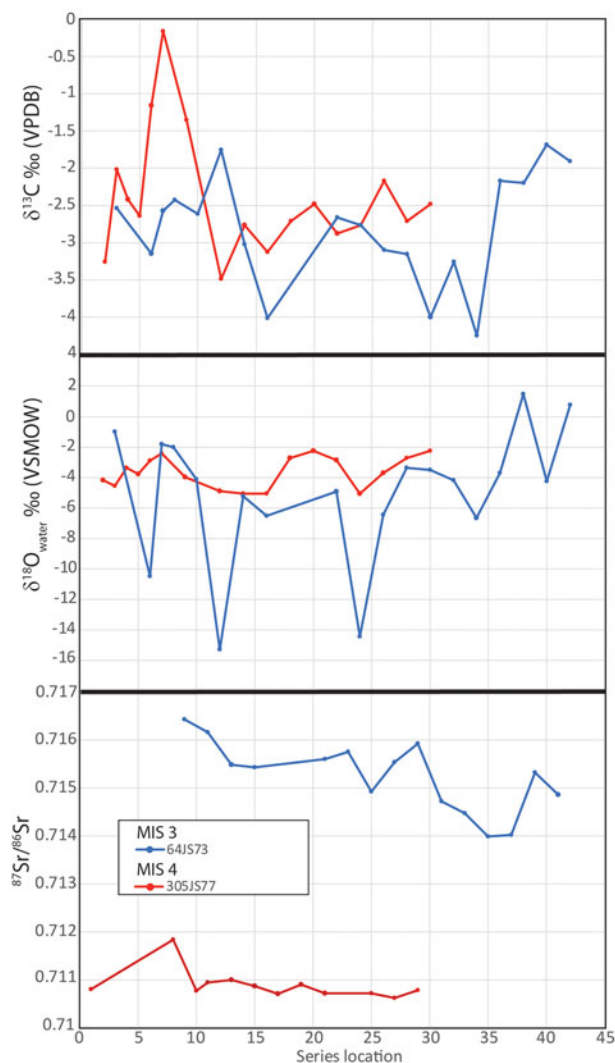
Figure 5. (color online) Time series, microsampled enamel $\delta^{13}C$, $\delta^{18}O$, and $^{87}Sr/^{86}Sr$. Both specimens are from Jones Spring, Hickory County, Missouri.
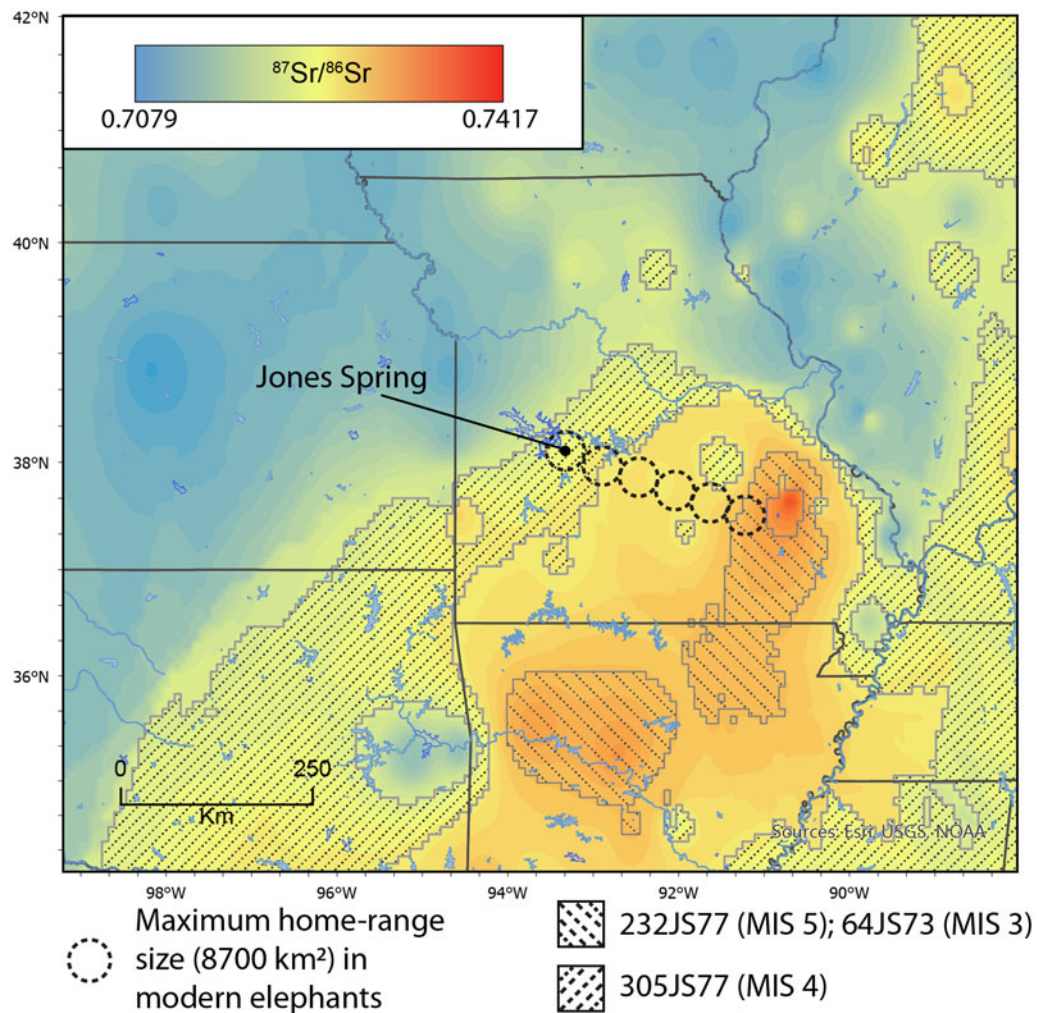
Figure 6. (color online) Mobility in mammoths from Jones Spring, Hickory County, Missouri. Hatched areas indicate the range of ^{87}Sr/^{86}Sr values from mammoth molar ridge-plates. One mammoth (305JS77) exhibits local values. Two separate mammoths (232JS77, 64JS73) exhibit Sr values, suggesting >200 km movement from the central core of the Ozark uplift. This implies movement over multiple years that is at least six times larger than the maximum home-range size documented for modern elephants in Etosha National Park, Namibia, Ngene et al. 2017. Basemap isoscape data are from Widga et al. (2017b) and Hedman et al. (2009, 2018).

Two mammoths from the Jones Spring site in southwest Missouri provide a pre–LGM perspective on landscapes that mammoths occupied (Fig. 4). A tooth-plate dating to MIS 5e from Jones Spring has less negative δ^{18}O and δ^{13}C values compared to the MIS 2 samples. This indicates warmer overall conditions and a diet that incorporated more C4 grasses throughout multiple years. Pollen from the same stratigraphic units further suggests that southwestern Missouri during MIS 5e was dominated by *Pinus* (no *Picea*) with a significant nonarboreal component (King, 1973). Importantly, Sr isotopes from this tooth indicate that while it was forming, the animal was foraging across surfaces that are more radiogenic than local values. The nearest area with ^{87}Sr/^{86}Sr values >0.7140 is the central Ozark uplift to the east of Jones Spring (Fig. 6). The wide amplitude of δ^{18}O values throughout the length of this tooth combined with the Sr isotope data indicating adherence to the central Ozark uplift suggest relatively broad shifts in annual water availability

or that this animal utilized a variety of water sources, including surface sources and freshwater springs.

The MIS 4 molar from Jones Spring has δ^{18}O values intermediate between the MIS 2 samples and the MIS 5e sample, along with δ^{13}C values that indicate more C4 consumption than MIS 2 samples (Fig. 4). This mammoth occupied a cooler environment than the MIS 5e mammoth, but it was significantly warmer than that of the late Pleistocene mammoths in the MIS 2 group.

In the case of the two microsampled mammoths from Jones Spring, isotopic trends in each animal illustrate different life histories (Fig. 5). The MIS 4 mammoth occupied the western Ozarks, as indicated by ^{87}Sr/^{86}Sr values deposited throughout the development of the sampled portion of the tooth. It occupied a landscape where C4 vegetation was common, with mild winter temperatures. The MIS 3 mammoth occupied the central core of the Ozark uplift, as indicated by ^{87}Sr/^{86}Sr values deposited during the formation of the
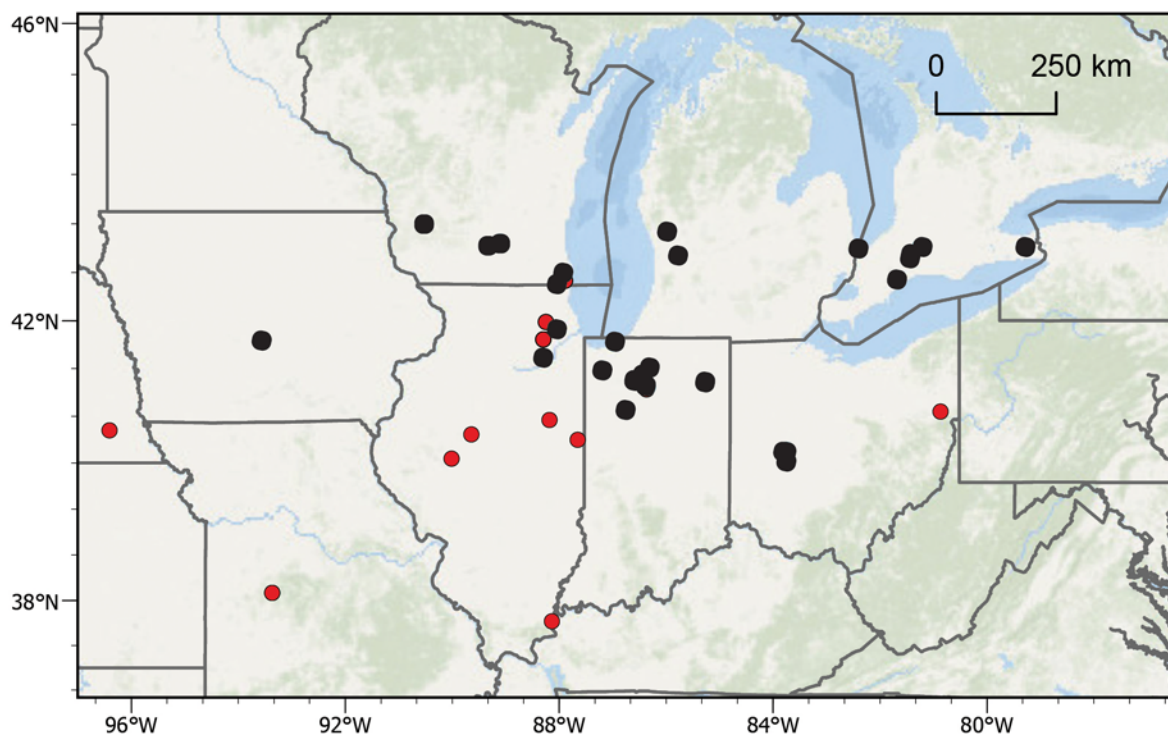
Figure 7. Distribution of mastodons with associated $\delta^{15}N_{coll}$ <5‰ data (black circles) and $\delta^{15}N_{coll}$ >5‰ data (red circles) during the Bølling-Allerød. (For interpretation of the references to color in this figure legend, the reader is referred to the web version of this article.)

sampled tooth. However, between the cessation of enamel formation and death, this animal moved ~200 km to the western Ozarks, where it was preserved in the Jones Spring deposits. The $\delta^{18}O$ series of this animal suggests greater seasonality during MIS 3 compared to MIS 5e, with deep negative excursions during the cold season. It also had a diet composed primarily of C4 vegetation.

These results suggest a broadly similar geographic scale of landscape use in late Quaternary mammoths in the Midwest to mammoths in the Great Plains and Florida (Hoppe et al., 1999; Hoppe, 2004; Esker et al., 2019). Overall, mammoths from both regions do not engage in significant seasonal migrations but can move greater distances at annual to decadal timescales. Further, although $\delta^{13}C_{coll}$ values in mammoths clearly suggest a niche that at times included C3-rich diets in a region that was dominated by forest, not grasslands, both Jones Spring mammoths were mixed feeders, with C4 grasses making up a significant part of their diet. The individual life histories of these mammoths were highly variable, underscoring the need to control for individual mobility in stable isotope studies of large herbivore taxa.

Testing scenarios of late Pleistocene proboscidean population dynamics

Can this stable isotope dataset illuminate trends in late Proboscidean population dynamics during deglaciation in the Midwest? It is possible that the shift in $\delta^{15}N$ represents the colonization of a novel ecological niche that also coincides

with climate and vegetation changes at the beginning of the Bølling-Allerød. However, it is unclear what this niche might be. Stable isotopes alone do not adequately define this niche space, and further paleobotanical work is necessary. Drucker et al. (2018) also noted anomalously low $\delta^{15}N$ values in LGM mammoths from Mezyhrich in central Europe and attributed this pattern to a large, but unspecific, shift in dietary niche. This is counter-intuitive in warming landscapes of the Midwest, since boreal forests typically have increased amounts of N-fixing microbes relative to tundra environments, thus increasing the $\delta^{15}N$ in forage overall.

Some studies have suggested that the growth rate of an individual is inversely correlated with $\delta^{15}N$ (Warinner and Tuross, 2010). This would be consistent with some scenarios of late Pleistocene mastodon population dynamics. Fisher (2009, 2018) suggests that predator pressure from Paleoindian groups who were megafaunal specialists would have caused mastodons to mature at a younger age. A decrease in the age at weaning would mean a shorter period of nursing-related elevated dietary $\delta^{15}N$ in young mastodons. If this were the case, we would expect an overall decrease in $\delta^{15}N$ of bone collagen in animals in their first and second decade of life. In our dataset, there is no significant change in maximum or mean $\delta^{15}N$ in mastodon bone collagen, despite a subset of mastodons that have lower $\delta^{15}N$ values. If predator pressure is contributing to faster maturation and shortening the time of nursing, then it is only occurring in some areas. However, even if this were the case in these areas, it is still uncertain what ecological processes might drive an increase in growth rate. Depending on local forage conditions experienced by an

animal, an increase in growth rate may be caused by increased predator pressure (Fisher, 2009) or a decrease in population density (Wolverton et al., 2009).

It is also possible that low $\delta^{15}N$ values in post-LGM mastodons represent a systematic change in predator avoidance strategies among some mastodon populations (Fiedel et al., 2019). Mastodons may have been attracted to low $\delta^{15}N$ areas such as marshes and wetlands as a response to new predators on the landscape (i.e., humans). However, taphonomic modification of late Pleistocene proboscidean materials by humans or other predators is extremely rare in this dataset (Widga et al., 2017a), so we see this scenario as an unlikely driver of mastodon landscape use.

In times when populations are dense on the landscape (Widga et al., 2017a) there may also be rapid, significant, and long-term changes to the N cycle. An influx of N via urea, as would be expected in high-density areas, would cause isotopically heavy plant roots and isotopically light shoots. Under intense grazing pressure, changes to N contributions change quickly from inorganic soil mineral N reservoirs to N from urea (McNaughton et al., 1988; Knapp et al., 1999). Individuals with lower $\delta^{15}N_{coll}$ values during the Allerød lived in areas with high mastodon populations, which may have contributed to isotopically light forage (due to ammonia volitization; see Knapp et al., 1999). However, this scenario does not explain why this shift is absent in our mammoth data during this time.

CONCLUSIONS

Stable isotopes of proboscidean tissues in midwestern North America illustrate the variability inherent in modern paleoecological analyses. Traditional approaches to understanding animal diets and landscape use through morphology and a reliance on modern analogues is inadequate for understanding paleoecological changes in megafaunal populations or during times of rapid ecological change, such as the late Quaternary.

Stable isotopes from bone collagen of midwestern proboscideans suggest consistently C3-dominated diets over the last 50 ka. During the LGM, mammoth diets may have included C3 grasses, but the prevalence of C3 flora during the post-LGM period is likely due to a landscape shift to more forest (Gonzales and Grimm, 2009; Saunders et al., 2010), with grasses making up very little of the floral communities in the southern Great Lakes region.

Despite the strong C3-signal in mammoth and mastodon diets during this period, the range of dietary flexibility and the degree of overlap between these two taxa is striking. The isotopically defined dietary niche of mammoths and mastodons shows increasing overlap as they approach extinction. Niche overlap is also supported by assemblages where both taxa co-occur (Saunders et al., 2010; Widga et al., 2017a). However, there are exceptions to this pattern, and some late mastodons exhibit low $\delta^{15}N$ values that may indicate the evolution and occupation of a new dietary niche, physiological responses to late Pleistocene ecological changes, or some other process acting on late mastodon populations.

Further resolution of mammoth and mastodon life histories are gleaned from stable isotopes in tooth enamel. $\delta^{13}C$ and $\delta^{18}O$ generally track climate and landscape changes experienced during tooth formation. MIS 2 mammoths are broadly similar in their isotopic life histories and illustrate relative homogeneity of landscape conditions across the Midwest at this time. Microsampled mammoth molars from Jones Spring, Missouri, indicate a significant increase in MIS 3 seasonality compared to MIS 4. Finally, some mammoths in this study died >200 km from where they lived during the formation of sampled molars, suggesting that lifetime mobility patterns in mammoths could have a significant effect on presumed "local" stable isotope values.

ACKNOWLEDGMENTS

SUPPLEMENTARY MATERIAL

The supplementary material for this article can be found at https://doi.org/10.1017/qua.2020.85

REFERENCES

Alroy, J., 2001. A multispecies overkill simulation of the end-Pleistocene megafaunal mass extinction. *Science* 292, 1893–1896.

Arppe, L., Karhu, J.A., Vartanyan, S., Drucker, D.G., Etu-Sihvola, H., Bocherens, H., 2019. Thriving or surviving? The isotopic record of the Wrangel Island woolly mammoth population. *Quaternary Science Reviews* 222, 105884.

Augustine, D.J., McNaughton, S.J., Frank, D.A., 2003. Feedbacks between soil nutrients and large herbivores in a managed savanna ecosystem. *Ecological Applications* 13, 1325–1337.

Austin, A.T., Vitousek, P.M., 1998. Nutrient dynamics on a precipitation gradient in Hawai'i. *Oecologia* 113, 519–529.

Bataille, C.P., Bowen, G.J., 2012. Mapping 87Sr/86Sr variations in bedrock and water for large scale provenance studies. *Chemical Geology* 304–305, 39–52.

Baumann, E.J., Crowley, B.E., 2015. Stable isotopes reveal ecological differences amongst now-extinct proboscideans from the Cincinnati region, USA. *Boreas* 44, 240–254.

Birks, H.H., van Geel, B., Fisher, D.C., Grimm, E.C., Kuijper, W.J., van Arkel, J., van Reenen, G.B.A., 2019. Evidence for the diet and habitat of two late Pleistocene mastodons from the Midwest, USA. *Quaternary Research* 91, 792–812.

Bocherens, H., Pacaud, G., Lazarev, P.A., Mariotti, A., 1996. Stable isotope abundances (13C, 15N) in collagen and soft tissues from

Pleistocene mammals from Yakutia: implications for the palae-obiology of the mammoth steppe. *Palaeogeography, Palaeoclimatology, Palaeoecology* 126, 31–44.

Brock, F., Higham, T., Ditchfield, P., Bronk Ramsey, C., 2010. Current pretreatment methods for AMS radiocarbon dating at the Oxford Radiocarbon Accelerator Unit (Orau). *Radiocarbon* 52, 103–112.

Bronk Ramsey, C., 2009. Bayesian analysis of radiocarbon dates. *Radiocarbon* 51, 337–360.

Broughton, J.M., Weitzel, E.M., 2018. Population reconstructions for humans and megafauna suggest mixed causes for North American Pleistocene extinctions. *Nature Communications* 9, 5441.

Bryant, D.J., Froelich, P.N., 1995. A model of oxygen isotope fractionation in body water of large mammals. *Geochimica et Cosmochimica Acta* 59, 4523–4537.

Cerling, T.E., Wittemyer, G., Ehleringer, J.R., Remien, C.H., Douglas-Hamilton, I., 2009. History of animals using isotope records (HAIR): a 6-year dietary history of one family of African elephants. *Proceedings of the National Academy of Sciences* 106, 8093–8100.

Chafota, J., Owen-Smith, N., 2009. Episodic severe damage to canopy trees by elephants: interactions with fire, frost and rain. *Journal of Tropical Ecology* 25, 341–345.

Coe, M., 1978. The decomposition of elephant carcasses in the Tsavo (East) National Park, Kenya. *Journal of Arid Environments* 1, 71–86.

Coltrain, J.B., Harris, J.M., Cerling, T.E., Ehleringer, J.R., Dearing, M.D., Ward, J., Allen, J. 2004. Rancho La Brea stable isotope biogeochemistry and its implications for the palaeoecology of late Pleistocene, coastal southern California. *Palaeogeography, Palaeoclimatology, Palaeoecology* 205, 199–219.

Daux, V., Lécuyer, C., Héran, M.A., Amiot, R., Simon, L., Fourel, F., Martineau, F., *et al.*, 2008. Oxygen isotope fractionation between human phosphate and water revisited. *Journal of Human Evolution* 55, 1138–1147.

Davis, M., Pineda-Munoz, S., 2016. The temporal scale of diet and dietary proxies. *Ecology and Evolution* 6, 1883–1897.

Delcourt, H.R., Delcourt, P., 1991. *Quaternary Ecology: A Paleoecological Perspective*. Chapman & Hall, New York.

Denny, M.W., Helmuth, B., Leonard, G.H., Harley, C.D.G., Hunt, L.J.H., Nelson, E.K., 2004. Quantifying scale in ecology: lessons from a wave-swept shore. *Ecological Monographs* 74, 513–532.

Dirks, W., Bromage, T.G., Agenbroad, L.D., 2012. The duration and rate of molar plate formation in *Palaeoloxodon cypriotes* and *Mammuthus columbi* from dental histology. *Quaternary International* 255, 79–85.

Drucker, D.G., Bridault, A., Iacumin, P., Bocherens, H., 2009. Bone stable isotopic signatures (15N, 18O) as tracers of temperature variation during the late glacial and early Holocene: case study on red deer *Cervus elaphus* from Rochedane (Jura, France). *Geological Journal* 44, 593–604.

Drucker, D.G., Stevens, R.E., Germonpré, M., Sablin, M.V., Péan, S., Bocherens, H., 2018. Collagen stable isotopes provide insights into the end of the mammoth steppe in the central east European Plains during the Epigravettian. *Quaternary Research* 90, 457–469.

El Adli, J.J., Cherney, M.D., Fisher, D.C., Harris, J.M., Farrell, A., Cox, S., 2015. Last years of life and season of death of a Columbian mammoth from Rancho La Brea. *Science Series, Natural History Museum of Los Angeles County* 42, 65–80.

El Adli, J.J., Fisher, D.C., Vartanyan, S.L., Tikhonov, A.N., 2017. Final years of life and seasons of death of woolly mammoths from Wrangel Island and mainland Chukotka, Russian Federation. *Quaternary International* 445, 135–45.

Esker, D., Forman, S.L., Widga, C., Walker, J.D., Andrew, J.E., 2019. Home range of the Columbian mammoths (*Mammuthus columbi*) and grazing herbivores from the Waco Mammoth National Monument (Texas, USA) based on strontium isotope ratios from tooth enamel bioapatite. *Palaeogeography, Palaeoclimatology, Palaeoecology* 534, 109291.

Feranec, R.S., Hadly, E.A., Paytan, A., 2009. Stable isotopes reveal seasonal competition for resources between late Pleistocene bison (*Bison*) and horse (*Equus*) from Rancho La Brea, southern California. *Palaeogeography, Palaeoclimatology, Palaeoecology* 271, 153–160.

Fiedel, S., Feranec, R., Marino, T., Driver, D., 2019. A new AMS radiocarbon date for the Ivory Pond mastodon. *Eastern Paleontologist* 3, 1–15.

Fisher, D.C., 2018. Paleobiology of Pleistocene proboscideans. *Annual Review of Earth and Planetary Sciences* 46, 229–260.

Fisher, D.C., 2009. Paleobiology and extinction of proboscideans in the Great Lakes region of North America. In: Haynes, G. (Ed.), *American Megafaunal Extinctions at the End of the Pleistocene*. Springer, Dordrecht, Netherlands, pp. 55–75.

Fisher, D.C., Fox, D.L., 2006. Five years in the life of an Aucilla River mastodon. In Webb, S.D. (Ed.), *First Floridians and Last Mastodons: The Page-Ladson Site in the Aucilla River*. Springer Dordrecht, Netherlands, pp. 343–377.

Fisher, D.C., Tikhonov, A.N., Kosintsev, P.A., Rountrey, A.N., Buigues, B., van der Plicht, J., 2012. Anatomy, death, and preservation of a woolly mammoth (*Mammuthus primigenius*) calf, Yamal Peninsula, northwest Siberia. *Quaternary International* 255, 94–105.

Fortelius, M., Solounias, N., 2000. Functional characterization of ungulate molars using the abrasion-attrition wear gradient: a new method for reconstructing paleodiets. *American Museum Novitates* 225, 1–36.

Fox-Dobbs, K., Bump, J.K., Peterson, R.O., Fox, D.L., Koch, P.L., 2007. Carnivore-specific stable isotope variables and variation in the foraging ecology of modern and ancient wolf populations: case studies from Isle Royale, Minnesota, and La Brea. *Canadian Journal of Zoology* 85, 458–471.

Fox-Dobbs, K., Leonard, J.A., Koch, P.L., 2008. Pleistocene megafauna from eastern Beringia: paleoecological and paleoenvironmental interpretations of stable carbon and nitrogen isotope and radiocarbon records. *Palaeogeography, Palaeoclimatology, Palaeoecology* 261, 30–46.

Fox, D.L., Fisher, D.C., 2001. Stable isotope ecology of a late Miocene population of *Gomphotherium productus* (Mammalia, Proboscidea) from Port of Entry Pit, Oklahoma, USA. *PALAIOS* 16, 279–293.

Frank, D.A., David Evans, R., Tracy, B.F., 2004. The role of ammonia volatilization in controlling the natural ^{15}N abundance of a grazed grassland. *Biogeochemistry* 68, 169–178.

Fujiyoshi, L., Sugimoto, A., Tsukuura, A., Kitayama, A., Lopez Caceres, M.L., Mijidsuren, B., Saraadanbazar, A., *et al.*, 2017. Spatial variations in larch needle and soil δ ^{15}N at a forest–grassland boundary in northern Mongolia. *Isotopes in Environmental and Health Studies* 53, 54–69.

Gill, J.L., Williams, J.W., Jackson, S.T., Lininger, K.B., Robinson, G.S., 2009. Pleistocene megafaunal collapse, novel plant communities, and enhanced fire regimes in North America. *Science* 326, 1100–1103.

Gonzales, L.M., Grimm, E.C., 2009. Synchronization of late-glacial vegetation changes at Crystal Lake, Illinois, USA with

the North Atlantic Event stratigraphy. *Quaternary Research* 72, 234–245.

Green, J.L., DeSantis, L.R.G., Smith, G.J., 2017. Regional variation in the browsing diet of Pleistocene *Mammut americanum* (Mammalia, Proboscidea) as recorded by dental microwear textures. *Palaeogeography, Palaeoclimatology, Palaeoecology* 487, 59–70.

Guldemond, R., Van Aarde, R., 2008. A meta-analysis of the impact of African elephants on savanna vegetation. *The Journal of Wildlife Management* 72, 892–899.

Handley, L.L., Raven, J.A., 1992. The use of natural abundance of nitrogen isotopes in plant physiology and ecology. *Plant, Cell and Environment* 15, 965–985.

Haynes, C.V., 1985. *Mastodon-bearing springs and late Quaternary geochronology of the Lower Pomme de Terre Valley, Missouri* (Vol. 204). Geological Society of America.

Hedges, R.E.M., Clement, J.G., David, C.,. Thomas, L., O'Connell, T.C., 2007. Collagen turnover in the adult femoral mid-shaft: modeled from anthropogenic radiocarbon tracer measurements. *American Journal of Physical Anthropology* 133, 808–816.

Hedman, K.M., Brandon Curry, B., Johnson, T.M., Fullagar, P.D., Emerson, T.E., 2009. Variation in strontium isotope ratios of archaeological fauna in the midwestern United States: a preliminary study. *Journal of Archaeological Science* 36, 64–73.

Hedman, K.M., Slater, P.A., Fort, M.A., Emerson, T.E., Lambert, J.M., 2018. Expanding the strontium isoscape for the American midcontinent: identifying potential places of origin for Cahokian and pre-Columbian migrants. *Journal of Archaeological Science: Reports* 22, 202–213.

Higgins, P., MacFadden, B.J., 2004. "Amount effect" recorded in oxygen isotopes of late glacial horse (*Equus*) and bison (*Bison*) teeth from the Sonoran and Chihuahuan deserts, southwestern United States. *Palaeogeography, Palaeoclimatology, Palaeoecology* 206, 337–353.

Higham, T F G, Jacobi, R.M., Bronk Ramsey, C., 2006. AMS radiocarbon dating of ancient bone using ultrafiltration. *Radiocarbon* 48, 179–195.

Hobbie, E.A., Macko, S.A., Williams, M., 2000. Correlations between foliar Δ15N and nitrogen concentrations may indicate plant-mycorrhizal interactions. *Oecologia* 122, 273–283.

Hoppe, K.A., 2004. Late Pleistocene mammoth herd structure, migration patterns, and Clovis hunting strategies inferred from isotopic analyses of multiple death assemblages. *Paleobiology* 30, 129–145.

Hoppe, K.A., Koch, P.L., 2007. Reconstructing the migration patterns of late Pleistocene mammals from northern Florida, USA. *Quaternary Research* 68, 347–352.

Hoppe, K.A., Koch, P.L., Carlson, R.W., Webb, S.D., 1999. Tracking mammoths and mastodons: reconstruction of migratory behavior using strontium isotope ratios. *Geology* 27, 439–442.

Iacumin, P., Di Matteo, A., Nikolaev, V., Kuznetsova, T.V., 2010. Climate information from C, N and O stable isotope analyses of mammoth bones from northern Siberia. *Quaternary International* 212, 206–212.

Keenan, S.W., Widga, C., Debruyn, J., Schaeffer, S., 2018. Nutrient hotspots through time: a field guide to modern and fossil taphonomy in east Tennessee. In: Engel, A.S., Hatcher, R.D., *Geology at Every Scale: Field Excursions for the 2018 GSA Southeastern Section Meeting in Knoxville, Tennessee*. Geological Society of America, Boulder, CO, pp. 61–74.

King, J.E., 1973. Late Pleistocene palynology and biogeography of the western Missouri Ozarks. *Ecological Monographs* 43, 539–565.

Knapp, A.K., Blair, J.M., Briggs, J.M., Collins, S.L., Hartnett, D.C., Johnson, L.C., Towne, E.G., *et al.*, 1999. The keystone role of bison in American tallgrass prairie: bison increase habitat heterogeneity and alter a broad plant, community, and ecosystem processes. *BioScience* 49, 39–50.

Koch, P.L., Hoppe, K.A., Webb, S.D., 1998. The isotopic ecology of late Pleistocene mammals in North America: part 1. Florida. *Chemical Geology* 152, 119–138.

Koch, P.L., Tuross, N., Fogel, M.L., 1997. The effects of sample treatment and diagenesis on the isotopic integrity of carbonate in biogenic hydroxylapatite. *Journal of Archaeological Science* 24, 417–429.

Lepper, B.T., Frolking, T.A., Fisher, D.C., Goldstein, G., Sanger, J.E., Wymer, D.A., Ogden, J.G., *et al.*, 1991. Intestinal contents of a late Pleistocene mastodon from midcontinental North America. *Quaternary Research* 36, 120–125.

McNaughton, S.J., Ruess, R.W., Seagle, S.W., 1988. Large mammals and process dynamics in African ecosystems. *BioScience* 38, 794–800.

Metcalfe, J.Z., Longstaffe, F.J., 2012. Mammoth tooth enamel growth rates inferred from stable isotope analysis and histology. *Quaternary Research* 77, 424–432.

Metcalfe, J.Z., Longstaffe, F.J., 2014. Environmental change and seasonal behavior of mastodons in the Great Lakes region inferred from stable isotope analysis. *Quaternary Research* 82, 366–377.

Metcalfe, J.Z., Longstaffe, F.J., Ballenger, J.A.M., Haynes, C.V., 2011. Isotopic paleoecology of Clovis mammoths from Arizona. *Proceedings of the National Academy of Sciences* 108, 17916–17920.

Metcalfe, J.Z., Longstaffe, F.J., Hodgins, G., 2013. Proboscideans and paleoenvironments of the Pleistocene Great Lakes: landscape, vegetation, and stable isotopes. *Quaternary Science Reviews* 76, 102–113.

Michelsen, A., Quarmby, C., Sleep, D., Jonasson, S., 1998. Vascular plant ^{15}N natural abundance in heath and forest tundra ecosystems is closely correlated with presence and type of mycorrhizal fungi in roots. *Oecologia* 115, 406–418.

Mosimann, J.E., Martin, P.S., 1975. Simulating overkill by Paleoindians: did Man hunt the giant mammals of the New World to extinction? Mathematical models show that the hypothesis is feasible. *American Scientist* 63, 304–313.

Newsom, L.A., Mihlbachler, M.C., 2006. Mastodons (*Mammut americanum*) diet foraging patterns based on analysis of dung deposits. In Webb, S.D., (Ed.), *First Floridians and Last Mastodons: The Page-Ladson Site in the Aucilla River*. Springer, Dordrecht, Netherlands, pp. 263–331.

Ngene, S., Okello, M.M., Mukeka, J., Muya, S., Njumbi, S., Isiche, J., 2017. Home range sizes and space use of African elephants (*Loxodonta africana*) in the southern Kenya and northern Tanzania borderland landscape. *International Journal of Biodiversity and Conservation* 9, 9–26.

Nogués-Bravo, D., Rodríguez, J., Hortal, J., Batra, P., Araújo, M.B., 2008. Climate change, humans, and the extinction of the woolly mammoth. *PLOS Biology* 6, e79.

Owen-Smith, R.N., 1992. *Megaherbivores: The Influence of Very Large Body Size on Ecology*. Cambridge University Press, Cambridge, UK.

Pacher, M., Stuart, A.J., 2009. Extinction chronology and palaeobiology of the cave bear (*Ursus spelaeus*). *Boreas* 38, 189–206.

Pérez-Crespo, V.A., Schaaf, P., Solís-Pichardo, G., Arroyo-Cabrales, J., Alva-Valdivia, L.M., Torres-Hernández, J.R., 2016. Strontium isotopes and mobility of a Columbian mammoth

(*Mammuthus columbi*) population, Laguna de las Cruces, San Luis Potosí, México. *Geological Magazine* 153, 743–749.

Plumptre, A.J., 1994. The effects of trampling damage by herbivores on the vegetation of the Pare National des Volcans, Rwanda. *African Journal of Ecology* 32, 115–129.

Rabanus-Wallace, M.T., Wooller, M.J., Zazula, G.D., Shute, E., Jahren, A.H., Kosintsev, P., Burns, J.A., *et al.*, 2017. Megafaunal isotopes reveal role of increase moisture on rangeland during late Pleistocene extinctions. *Nature Ecology & Evolution* 1, 0125.

Rasmussen, S.O., Bigler, M., Blockley, S.P., Blunier, T., Buchardt, S.L., Clausen, H.B., Cvijanovic. I., *et al.*, 2014. A stratigraphic framework for abrupt climatic changes during the last glacial period based on three synchronized Greenland ice-core records: refining and extending the INTIMATE event stratigraphy. *Quaternary Science Reviews* 106, 14–28.

Reimer, P. J., Bard, E., Bayliss, A., Beck, J. W., Blackwell, P. G., Bronk Ramsey, C., Buck, C. E., *et al.*., 2013. IntCal13 and Marine13 radiocarbon age calibration curves 0–50,000 years cal BP. *Radiocarbon* 55 (4), 1869-1887.

Rhodes, A.N., Urbance, J.W., Youga, H., Corlew-Newman, H., Reddy, C.A., Klug, M.J., Tiedje, J.M., *et al.*, 1998. Identification of bacterial isolates obtained from intestinal contents associated with 12,000-year-old mastodon remains. *Applied and Environmental Microbiology*. 64, 651–658.

Richards, M.P., Hedges, R.E.M., 2003. Variations in bone collagen $\delta^{13}C$ and $\delta^{15}N$ values of fauna from northwest Europe over the last 40,000 years. *Palaeogeography, Palaeoclimatology, and Palaeoecology* 193, 261–267.

Ripple, W.J., Van Valkenburgh, B., 2010. Linking top-down forces to the Pleistocene megafaunal extinctions. *BioScience* 60, 516–526.

Rountrey, A.N., Fisher, D.C., Tikhonov, A.N., Kosintsev, P.A., Lazarev, P.A., Boeskorov, G., Buigues, B., 2012. Early tooth development, gestation, and season of birth in mammoths. *Quaternary International* 255, 196–205.

Saunders, J.J., Grimm, E.C., Widga, C.C., Dennis Campbell, G., Curry, B.B., Grimley, D.A., Hanson, P.R., *et al.*, 2010. Paradigms and proboscideans in the southern Great Lakes region, USA. *Quaternary International* 217, 175–187.

Schubert, B.A., Jahren, A.H., 2015. Global increase in plant carbon isotope fractionation following the last glacial maximum caused by increase in atmospheric pCO2. *Geology* 43, 435–438.

Schulze, E.-D., Chapin, F.S., Gebauer, G., 1994. Nitrogen nutrition and isotope differences among life forms at the northern treeline of Alaska. *Oecologia* 100, 406–412.

Schwartz-Narbonne, R., Longstaffe, F.J., Kardynal, K.J., Druckenmiller, P., Hobson, K.A., Jass, C.N., Metcalfe, J.Z., *et al.*, 2019. Reframing the mammoth steppe: insights from analysis of isotopic niches. *Quaternary Science Reviews* 215, 1–21.

Shearer, G, Kohl, D., 1993. Natural abundance of 15N: fractional contribution of two sources to a common sink and use of isotope discrimination. In: Knowles, R., Blackburn, T.H. (Eds.), *Nitrogen Isotope Techniques*. Academic Press, San Diego, CA, pp. 89–125.

Slater, P.A., Hedman, K.M., Emerson, T.E., 2014. Immigrants at the Mississippian polity of Cahokia: strontium isotope evidence for population movement. *Journal of Archaeological Science* 44, 117–127.

Smith, G.J., DeSantis, L.R.G., 2018. Dietary ecology of Pleistocene mammoths and mastodons as inferred from dental microwear textures. *Palaeogeography, Palaeoclimatology, Palaeoecology* 492, 10–25.

Stevens, R., Jacobi, R., Street, M., Germonpre, M., Conard, N., Munzel, S., Hedges, R.E.M., 2008. Nitrogen isotope analyses of reindeer (*Rangifer tarandus*), 45,000 BP to 9,000 BP: palaeoenvironmental reconstructions. *Palaeogeography, Palaeoclimatology, Palaeoecology* 262, 32–45.

Stuart, A.J., 2015. Late Quaternary megafaunal extinctions on the continents: a short review. *Geological Journal* 50, 338–363.

Stuart, A.J., Kosintsev, P.A., Higham, T.F.G., Lister, A.M., 2004. Pleistocene to Holocene extinction dynamics in giant deer and woolly mammoth. *Nature* 431, 684.

Stuart, A.J., Lister, A.M., 2011. Extinction chronology of the cave lion *Panthera spelaea*. *Quaternary Science Reviews*, 30, 2329–2340.

Stuart, A.J., Lister, A.M., 2012. Extinction chronology of the woolly rhinoceros *Coelodonta antiquitatis* in the context of late Quaternary megafaunal extinctions in northern Eurasia. *Quaternary Science Reviews* 51, 1–17.

Surovell, T.A., Pelton, S.R., Anderson-Sprecher, R., Myers, A.D., 2016. Test of Martin's overkill hypothesis using radiocarbon dates on extinct megafauna. *Proceedings of the National Academy of Sciences* 113, 886–891.

Surovell, T., Waguespack, N., Brantingham, P.J., 2005. Global archaeological evidence for proboscidean overkill. *Proceedings of the National Academy of Sciences* 102, 6231–6236.

Szpak, P., Gröcke, D.R., Debruyne, R., MacPhee, R.D.E., Guthrie, R.D., Froese, D., Zazula, G.D., *et al.*, 2010. Regional differences in bone collagen $\delta^{13}C$ and $\delta^{15}N$ of Pleistocene mammoths: implications for paleoecology of the mammoth steppe. *Palaeogeography, Palaeoclimatology, Palaeoecology* 286, 88–96.

Teale, C.L., Miller, N.G., 2012. Mastodon herbivory in midlatitude late-Pleistocene boreal forests of eastern North America. *Quaternary Research* 78, 72–81.

Tuross, N., Fogel, M.L., Hare, P.E., 1988. Variability in the preservation of the isotopic composition of collagen from fossil bone. *Geochimica et Cosmochimica Acta* 52, 929–935.

Uno, K.T., Quade, J., Fisher, D.C., Wittemyer, G., Douglas-Hamilton, I., Andanje, S., Omondi, P., *et al.*, 2013. Bomb-curve radiocarbon measurement of recent biologic tissues and applications to wildlife forensics and stable isotope (paleo)ecology. *Proceedings of the National Academy of Sciences* 110, 11736–11741.

Valeix, M., Fritz, H., Sabatier, R., Murindagomo, F., Cumming, D., Duncan, P., 2011. Elephant-induced structural changes in the vegetation and habitat selection by large herbivores in an African savanna. *Biological Conservation* 144, 902–912.

van Geel, B., Fisher, D.C., Rountrey, A.N., van Arkel, J., Duivenvoorden, J.F., Nieman, A.M., van Reenen, G.B.A., *et al.*, 2011. Palaeo-environmental and dietary analysis of intestinal contents of a mammoth calf (Yamal Peninsula, northwest Siberia). *Quaternary Science Reviews* 30, 3935–3946.

Warinner, C., Tuross, N., 2010. Brief communication: tissue isotopic enrichment associated with growth depression in a pig: implications for archaeology and ecology. *American Journal of Physical Anthropology* 141, 486–493.

Widga, C., Lengyel, S.N., Saunders, J., Hodgins, G., Walker, J.D., Wanamaker, A.D., 2017a. Late Pleistocene proboscidean population dynamics in the North American midcontinent. *Boreas* 46, 772–782.

Widga, C., Walker, J.D., Boehm, A., 2017b. Variability in bioavailable $^{87}Sr/^{86}Sr$ in the North American midcontinent. *Open Quaternary* 3, 4.

Widga, C., Walker, J.D., Stockli, L.D., 2010. Middle Holocene bison diet and mobility in the eastern Great Plains (USA) based on δ13C, δ18O, and 87Sr/86Sr analyses of tooth enamel carbonate. *Quaternary Research* 73, 449–463.

Wolverton, S., Lyman, R.L., Kennedy, J.H., La Point, T.W., 2009. The terminal Pleistocene extinctions in North America, hypermorphic evolution, and the dynamic equilibrium model. *Journal of Ethobiology* 29, 28–63.

Yansa, C.H. and Adams, K.M., 2012. Mastodons and mammoths in the Great Lakes region, USA and Canada: New insights into their diets as they neared extinction. *Geography Compass* 6, 175–188.

Zazzo, A., Balasse, M., Patterson, W.P., 2006. The reconstruction of mammal individual history: refining high-resolution isotope record in bovine tooth dentine. *Journal of Archaeological Science* 33, 1177–1187.